Published in final edited form as:
Dev Cell. 2011 January 18; 20(1): 131–139. doi:10.1016/j.devcel.2010.12.003.

MICROAUTOPHAGY OF CYTOSOLIC PROTEINS BY LATE ENDOSOMES

Ranjit Sahu[1], **Susmita Kaushik**[2], **Cristina C. Clement**[1], **Elvira S. Cannizzo**[1], **Brian Scharf**[1], **Antonia Follenzi**[1], **Ilaria Potolicchio**[1], **Edward Nieves**[2], **Ana Maria Cuervo**[2,4], and **Laura Santambrogio**[1,3,4]

[1]Department of Pathology, Albert Einstein College of Medicine, Bronx, NY, 10461, USA.

[2]Department of Developmental and Molecular Biology, Albert Einstein College of Medicine, Bronx, NY, 10461, USA.

[3]Department of Microbiology and Immunology, Albert Einstein College of Medicine, Bronx, NY, 10461, USA.

Summary

Autophagy delivers cytosolic components to lysosomes for their degradation. The delivery of autophagic cargo to late endosomes for complete or partial degradation has also been described. In this report, we present evidence that distinct autophagic mechanisms control cytosolic protein delivery to late endosomes and identify a microautophagy-like process that delivers soluble cytosolic proteins to the vesicles of late endosomes/multivesicular bodies (MVB). This microautophagy-like process has selectivity and is distinct from chaperone-mediated autophagy that occurs in lysosomes. Endosomal microautophagy occurs during MVB formation, relying on the ESCRT I and III systems for formation of the vesicles in which the cytosolic cargo is internalized. Protein cargo selection is mediated by the chaperone hsc70 and requires the cationic domain of hsc70 for electrostatic interactions with the endosomal membrane. Therefore, we propose that endosomal microautophagy shares molecular components with both the endocytic and autophagic pathways.

Introduction

Autophagy or the degradation of cytosolic components in lysosomes is a pathway utilized by all cell types as a means to overcome starvation, recycle nutrients and remove unwanted or damaged intracellular constituents including both proteins and organelles (Mizushima et al., 2008). In addition, delivery of autophagic cargo to late endosomes for complete or partial degradation has been described (Dengjel et al., 2005; Nimmerjahn et al., 2003). To date, three autophagy-related pathways have been described in higher eukaryotes: macroautophagy (MA), chaperone-mediated autophagy (CMA) and microautophagy (Cuervo, 2010; Mizushima et al., 2008). In MA, whole cytosolic regions are sequestered inside a vesicle (autophagosome) that then fuses with lysosomes or with late endosomal

[4]Corresponding authors: Laura Santambrogio: Albert Einstein College of Medicine, 1300 Morris Park Avenue, 10461 Bronx, New York, NY. laura.santambrogio@einstein.yu.edu tel, 718 430-3458. Ana Maria Cuervo: Albert Einstein College of Medicine, 1300 Morris Park Avenue, 10461 Bronx, New York, NY. ana-maria.cuervo@einstein.yu.edu.

multivesicular bodies (MVB) (Mizushima et al., 2008). CMA is a more selective autophagy that relies on the recognition by the hsc70 chaperone of amino acid motifs on cytosolic substrate proteins biochemically related to the pentapeptide KFERQ (Chiang et al., 1989; Dice, 1990). The complex hsc70/ cytosolic substrate binds to the lysosome-associated membrane protein type 2A (LAMP-2A) (Cuervo and Dice, 1996) and after unfolding substrate proteins are translocated into lysosomes for degradation assisted by a luminal form of hsc70 (Cuervo, 2010). A third autophagic pathway, microautophagy, has been described in yeast but has not yet been well characterized in eukaryotic cells (Marzella et al., 1981). This pathway involves internalization of cytosolic cargo through invaginations of the lysosomal membrane (Marzella et al., 1981), which resemble the formation of multivesicular bodies (MVB). The molecular mechanisms that mediate microautophagy-like delivery of cytosolic cargo to lysosomes in mammals remain unknown. The relationship between the invagination of the membrane during this process and MVB biogenesis is also not clear.

In this report, we have analyzed the autophagic mechanisms operating in late endosomal MVB comparatively to those active in lysosomes. Using a series of mutants, we present evidence that MA is operative in LE, whereas LAMP-2A-mediated CMA is not involved in cytosolic protein translocation in the MVB lumen or in the luminal vesicles. Instead, we provide evidence that a microautophagy-like process occurs during MVB biogenesis to deliver selected soluble cytosolic proteins to the vesicles of late endosomes/MVB. This process is mediated by chaperones, but in contrast to CMA that occurs in lysosomes, endosomal microautophagy: 1) relies on the ESCRT I and III complexes, required for the formation of the vesicles in which the cytosolic cargo is internalized, and 2) relies on protein cargo delivery by hsc70 through electrostatic interactions of this chaperone with the endosomal limiting membrane. Therefore, we propose that endosomal microautophagy shares molecular components with both the endocytic and autophagic pathways and contributes to degradation of the soluble cytosol.

Results and Discussion

Cytosolic proteins are delivered to both lysosomes and late endosomal compartments

To analyze potentially distinct autophagic pathways operating between lysosomes and LE in dendritic cells (DC), we used three soluble cytosolic proteins as target: glyceraldehyde-3-phosphate dehydrogenase (GAPDH) and aldolase, which possess the KFERQ-like targeting motif required for CMA (Aniento et al., 1993) and cyclophilin, which does not. Immunoblot of isolated subcellular organelles (Fig. S1) for these three proteins confirmed that, as described for other cells (Aniento et al., 1993), a fraction of the two proteins bearing the CMA-targeting motif – GAPDH and aldolase – was detected in CMA-active (CMA+) lysosomes, whereas their association to CMA-inactive (CMA−) lysosomes was negligible (Fig. 1A). In contrast, cyclophilin, which lacks the CMA-targeting motif, was detectable in both groups of lysosomes (Fig. 1A). The three proteins were present in the late endosomal (LE) fraction but almost undetectable in the fractions enriched in autophagosomes and autophagolysosomes (Fig. 1A).

The presence of the cytosolic proteins in LE and the abundance of hsc70 in this compartment led us to analyze whether direct translocation of cytosolic proteins occurs into LE and if it could be reproduced *in vitro*. To that purpose, we incubated LE and lysosomes with a pool of radiolabeled cytosolic proteins and tracked their degradation. Proteolysis in this *in vitro* system only occurs when the radiolabeled proteins reach the organelle lumen and, consequently it is a good indication of internalization (Kaushik and Cuervo, 2009). As previously described, CMA+ lysosomes showed the highest rates of internalization/ proteolysis while very low degradation was detected for CMA-inactive lysosomes (Fig. 1B).

Incubation of LE under the same conditions revealed rates of protein translocation/degradation in this fraction close to those detected in CMA+ lysosomes, and clearly higher than for the total pool of cellular lysosomes (formed by 20–30% CMA+ and 70% CMA- lysosomes) (Fig. 1B). Direct uptake of cytosolic proteins by LE is ATP-dependent (apyrase decreases internalization by 38.5%; Fig. 1C), but does not require GTP or GTP hydrolysis (Fig. 1C).

Although the three cytosolic soluble proteins were barely detectable in isolated autophagosomes (Fig. 1A), to directly analyze the contribution of MA to their delivery into LE, we used a genetic approach to block MA in DC by lentiviral-based shRNA for Atg7, an essential MA protein (Tanida et al., 1999) (Fig. 1D). Ultrastructural analysis confirmed that the typical double membrane autophagosomes observed in control cells (Fig. 1E) were not present in the Atg7 knock down cells (Atg7(−)) (autophagosomes/cell were 12+3.2 in control and 3.8+0.8 in Atg7(−) cells). No morphological differences in MVB or in lysosomal ultrastructure were observed between Atg7(−) and control cells (Fig. 1F). Immunoblot of isolated LE revealed a moderate decrease in the amount of the three cytosolic proteins in Atg7(−) cells (about 20% decrease; Fig. 1G and S2). These results indicate that autophagosome-mediated transport is also involved in delivery of cytosolic antigens to LE, but its contribution, at least under the conditions of our study, is quantitatively small. In fact, using similar *in vitro* delivery assays to the ones described in the previous section, we found that MA blockage did not affect the ability of LE to directly take up and degrade a pool of radiolabeled cytosolic proteins (Fig. 1H). Additionally, despite the 20% decrease in total endosomal GAPDH upon MA blockage, the amount of the same protein was increased inside the LE vesicles (secreted as exosomes) in these cells (Fig. 1I). Thus, our results indicate that part of the cytosolic proteins detected in LE reach this compartment by a pathway different from MA and that this process can be reproduced *in vitro*.

Delivery of cytosolic proteins to LE is independent of LAMP-2A but requires Vps4 and Tsg101-mediated MVB formation

We next investigated whether part of the cytosolic proteins detected in LE reached this compartment via CMA. Translocation of cytosolic proteins into lysosomes by CMA is directly reliant on recognition of a targeting sequence by cytosolic hsc70 that then delivers the cargo protein to lysosomal LAMP-2A (Bandyopadhyay et al., 2008; Cuervo and Dice, 1996). Knockdown of LAMP-2A to reduce CMA activity in DC resulted in a marked decrease in the levels of GAPDH and aldolase in CMA+ lysosomes (Fig. 1J). In contrast, none of the analyzed proteins was decreased in LE from LAMP-2A(−) cells (Fig. 1J). Ultrastructural analysis indicated no morphological differences in LE between control and LAMP-2A(−) DC (Fig. 1K). Using the *in vitro* assay, we observed a significant decrease in protein uptake/degradation in lysosomes but not LE of LAMP-2A(−) DC (Fig. 1L). Levels of GAPDH in LE prepared from LAMP-2A(−) fibroblasts were also comparable to control, supporting that LE uptake of cytosolic proteins is also independent of CMA in other cell types (Fig. 1M). These data confirm that LE internalization of soluble proteins does not take place through CMA or at least through the same type of CMA described in lysosomes.

A third mechanism for delivery of cytosolic components to lysosomes, known as microautophagy, has been characterized in yeast (Kunz et al., 2004) where it involves a cholesterol-dependent direct invagination of the vacuole membrane (equivalent to lysosomes) into the lumen followed by pinching off of the newly formed vesicles. Because this phenomenon resembles the biogenesis of vesicles in the MVB, we first investigated whether compromising vesiculation on MVB biogenesis would reduce cytosolic cargo transport into LE. The endosomal sorting complexes required for transport (ESCRT) are a series of cytosolic proteins recruited to the LE limiting membrane that control transport of

membrane-bound ubiquitinated proteins, as well as endosomal vesiculation (Saksena and Emr, 2009). We first targeted Vps4, an ATPase required to dissociate ESCRT from the endosomal membrane (Saksena and Emr, 2009). We used a mixture of shRNAs for the two Vps4 isoforms (A and B) at a MOI of 25 which would reduce Vps4 by 60% (Fig. 2A) without affecting cell survival (complete Vps4 knock-down compromised cell viability (data not shown)). Additionally, we also knocked down Tsg101, an ESCRT I protein positive regulator of MVB biogenesis (Falguieres et al., 2008) (Fig. 2B). Ultrastructural analysis of both Vps4(−) DC (Fig. 2C, D) and purified LE from these cells (Fig. 2E) confirmed that MVB structure was compromised as long elongated vesicular-like structures that fail to pinch-off from the limiting membrane were observed (Saksena and Emr, 2009). Immunoblot of organelles purified from control, Vps4(−) and Tsg101(−) cells revealed a decrease in the total amounts of cyclophilin, GAPDH and aldolase in LE but not in lysosomes (Fig. 2F, G). *In vitro* transport assays confirmed a significant decrease in uptake/degradation of the mixture of cytosolic radiolabeled proteins by LE but not in lysosomes (Fig. 2H). Furthermore, antibody-blockage of Vps4 in isolated control organelles significantly reduced uptake of cytosolic proteins by LE but not by lysosomes confirming the role of Vps4 in uptake in the former compartment (Fig. 2I). The fact that compromising formation of MVB structures affected LE uptake of the three individual cytosolic proteins analyzed and the pool of cytosolic protein, suggests that some level of “in bulk” non-selective microautophagy is taking place continuously during MVB biogenesis. In fact, in Vps4(−) DC expressing cytosolic GFP, LE transport of GFP was also reduced (Fig. 2J). Treatment of DC with U18666A to interfere with cholesterol trafficking (Liscum and Faust, 1989) disrupted the classical MVB morphology confirming that cholesterol is also required for LE microautophagy (Fig. 2K). Taken together, these data indicate that a portion of the soluble cytosolic proteome is being continuously trapped in LE vesicles during MVB biogenesis and that the contribution of this system is more relevant than MA for transport of soluble proteins into LE.

Immunogold labeling for GAPDH in MVB (Fig. 3A) and ultrastructural tomography (Fig. 3B) revealed that GAPDH is present both inside the MVB vesicles as well as in the lumen of LE. The GAPDH inside the vesicles could only reach this topology if sequestered from the cytosol as the vesicles derive from invagination of the LE limiting membrane. The GAPDH in the LE lumen could originate from either breakage/degradation of the vesicles or be delivered to this compartment by MA through fusion of autophagosomes and LE. To determine the fraction of the cytosolic proteome that reaches LE by each of these two pathways we performed proteomic analysis of cytosol compared to the soluble contents of purified autophagic vacuoles (AV) and exosomes (Fig. 3C). In AV, soluble cytosolic proteins represented 36% of the total content as opposed to a 66% present in exosomes (Fig. 3C, Table S1). Mitochondrial, cytoskeleton and ER-Golgi proteins were abundant in AV but poorly represented in exosomes (Fig. 3C). These differences were further confirmed by western blot analysis (Fig. 3D). Interestingly, quantification in cytosol, AV and exosomes of cytosolic soluble proteins expressing the KFERQ-like motif recognized by hsc70 for CMA targeting, indicated a selection for motif-expressing proteins in exosomes (75% in endosomes vs. only 37% in cytosol; Fig. 3E). These findings support that sequestration of cytosolic proteins by MVB displays selectivity toward KFERQ-containing proteins. Consequently, transport of soluble cytosolic proteins into MVB occurs in a microautophagy-like fashion that may involve both a non-selective engulfment of cytosolic proteins, but also a selective uptake of specific cytosolic proteins (KFERQ-containing proteins).

Selective microautophagy requires hsc70

The fact that transport of cytosolic proteins into LE was independent of LAMP-2A and required the formation of membrane invaginations suggested that it did not occur via CMA.

However, the enrichment in proteins containing KFERQ-like targeting motifs in the vesicles of MVB and in exosomes led us to investigate the possible participation of hsc70 in cargo delivery to LE. Because knock down of hsc70 selectively in the endocytic and lysosomal compartments is not possible, we instead incubated purified LE with antibodies against hsc70, Vps4, LAMP-2A or LAMP-2B and determined the cytosol-endosomes translocation efficiency for a pool of radiolabeled cytosolic proteins (Fig. 3F,G and S3). Blocking Vps4 or hsc70 reduced the amount of protein uptake/proteolysis in LE by 30 to 50% (Fig. 3F). The fact that incubation with both antibodies did not have an additive effect supports that Vps4 and hsc70 act in the same pathway, and that hsc70 is likely the limiting factor. No inhibitory effect was observed by blocking LAMP-2A or LAMP-2B, thus negating the contribution of CMA or steric hindrance of the antibodies at the surface of the organelle (Fig. 3F). The observed decrease in proteolysis was a result of reduced uptake rather than degradation, as incubation of disrupted LE with the antibody did not affect proteolytic activity (Fig. S3B). Sensitivity to hsc70 blockage was also detected for the uptake of cytosolic proteins into LE from mouse liver (Fig. S3 C,D), supporting the general nature of this process.

The involvement of hsc70 in LE microautophagy in a KFERQ-dependent manner was further confirmed in translocation assays with radiolabeled GAPDH and cyclophilin. We found that uptake/proteolysis of the KFERQ-containing protein (GAPDH) by LE was 4 times higher than that of cyclophilin that lacks this motif (Fig. 3G). Pre-incubation of LE with the antibody to hsc70, but not LAMP-2A, significantly reduced GAPDH uptake and proteolysis by LE but did not affect cyclophilin LE uptake (Fig. 3G). Last, we confirmed that the effect of hsc70 on LE translocation of cytosolic proteins requires binding of this chaperone to the KFERQ-like motif using DC expressing wild type or a mutant form of GAPDH lacking this motif (nrvvd to aavvd). As shown in Fig. 3H, the amount of mutated GAPDH detected in isolated LE was significantly lower when compared to the wild type form.

Hsc70 interaction with the endosomal compartments

We speculate that the need for hsc70 in LE microautophagy may be related to the unfolding ability of this chaperone as one of the essential requirements for CMA of cytosolic proteins in lysosomes is the need for their unfolding before they can cross the lysosomal membrane (Salvador et al., 2000). To determine whether protein unfolding was required for internalization of proteins in LE, we transfected DC with a plasmid expressing a form of dihydrofolate reductase (DHFR) that contains a KFERQ-like motif in its n-terminus (Salvador et al., 2000) (Fig. 4A). Stabilization of the conformation of DHFR with methotrexate (MTX) which prevents its unfolding did not affect the amount of DHFR detected in LE, supporting that unfolding is not required for its LE uptake (Fig. 4B).

Because LAMP-2A was not required for LE microautophagy, we set to determine whether hsc70-mediated translocation of cytosolic proteins into the LE vesicles depends on the interaction of this chaperone with the endosomal limiting membrane. Incubation of increasing amounts of hsc70 with purified LE labeled with 5-Octadecanoylamino fluorescein - a fluorescent probe sensitive to the fluidity and the physical/chemical composition of the membrane lipid bilayer – revealed an increase in hsc70 binding to LE with saturation at a 2:1 hsc70/LE protein ratio (Fig. 4C). The interaction was reversed by ATP addition (Fig. 4C, S4A) (Arispe and De Maio, 2000). To investigate the nature of the molecule(s) recruiting hsc-70 to LE we immunoprecipitated His-tagged hsc70 bound to isolated LE and analyzed the eluate by MS/MS analysis. Proteins known to be hsc-70 cytosolic cargo were detected (data not shown); however, none of the molecular species were integral components of the endosomal membrane that could be serving as receptors of hsc-70 in late endosomes. On the other hand when the eluate was analyzed by thin layer chromatography lipids could be detected (Fig. S4B). The immunoprecipitation was repeated

in presence or absence of ATP, since the latter inhibits hsc-70 endosomal binding (Fig. 4D). Analysis of the eluted lipids by multidimensional mass spectrometry scan (200–2000 m/z) analysis indicated the presence of PS (Fig. 4E and F).

Although hsc70 does not bear any of the canonical protein lipid-binding domain, its C terminal region (aa 526 to 539) presents one cluster of basic residues which could potentially bind to acidic phospholipids through electrostatic interaction (Fig. 4G) (Yeung et al., 2008). In addition, two clusters of hydrophobic side chains of amino acids are also present (Fig. 4G). This amphiphilic (cationic/hydrophobic) strategy is used by several biological structures to insert into anionic membranes and it was previously shown to be used by PS to recruit proteins to the endosomal limiting membrane (Yeung et al., 2008). Even though PS is distributed in all cellular membranes, it only confers a negative charge to the plasma and the endosomal membranes, likely because the PS present in mitochondria, Golgi and ER is confined to their luminal leaflets (Yeung et al., 2008). Discrimination of binding between the PS in plasma membrane and LE is probably mediated by the strength of the charge. It has been shown that PS directs proteins with strong positive charge to the cytosolic leaflet of the plasma membrane and proteins with moderate positive charge, such as hsc-70, to the cytosolic leaflet of the endosomal membrane (Yeung et al., 2008). Hence, to determine whether hsc70 utilizes this strategy, we generated a series of mutants where basic (K and R) amino acids were substituted with A to disrupt the positive surface charges (Fig. 4G). We then compared hsc-70 translocation into LE isolated from cells transfected with myc-tagged wild type hsc70 or the 533R/A, 535K/A, 539K/A mutants. Hsc-70 uptake was comparable to control for the 533R/A or 539K/A mutants, whereas a significant decrease of endosomal hsc-70 was observed in cells transfected with the 535K/A mutant (Fig. 4H). Accordingly, *in vitro* binding of this mutant hsc70, to purified LE was significantly reduced (Fig. 4I). Altogether, these results indicate that the anchoring of hsc70 to the endosomal anionic membrane requires its polybasic cluster.

In summary, we report that a portion of the soluble cytosolic proteome is continuously trapped in LE vesicles during MVB biogenesis. This microautophagy-like mechanism transports cytosolic proteins into LE but not lysosomes in a chaperone-dependent manner. This process does not require substrate unfolding or the essential component of CMA in lysosomes, LAMP-2A, but it relies on electrostatic binding of hsc70 to endosomal acidic phospholipids. Although some level of microautophagy of cytosolic proteins can occur independently of hsc70, binding to the chaperone may mediate preferential enrichment of a particular subset of cytosolic proteins in MVB and confer selectivity to this process. Importantly, cytosolic proteins that access MVB through MA or microautophagy constitute two separate pools. MA-mediated transport occurs by fusion of the autophagosome with the organelle limiting membrane and directly delivers cytosolic proteins and organelles to the lumen of the compartment where the processing enzymes are available. In contrast, microautophagy delivers the majority of cytosolic proteins into the vesicle lumen. Some of these vesicles may undergo degradation directly in LE, because we could detect proteolysis of the cytosolic proteins internalized by microautophagy. Altogether, these two dedicated systems allow degradation of both the soluble cytosol as well as subcellular organelles.

Experimental Procedures

Cells and treatments

Dendritic cells (JAWS) were grown to confluence in DMEM media with HI-FBS. U18666A and methotrexate were added directly to the culture media for 48h and 16h, respectively (see Supplemental Experimental Procedures for details).

Isolation of organelles and cytosol

Late endosomes and lysosomes were isolated using centrifugation in Percoll gradients (Castellino and Germain, 1995), secondary lysosomes using a discontinuous gradient of metrizamide (Wattiaux et al., 1978), and autophagic vacuoles and mitochondria using a different discontinuous gradient of metrizamide (Marzella et al., 1981). Where indicated, two groups of lysosomes with high (CMA+) and low (CMA−) activity for CMA were isolated by the method described in (Cuervo et al., 1997). Exosomes were prepared as previously reported (Potolicchio et al., 2005). ER and cytosol were obtained in the pellet and supernatant respectively, after centrifugation at 100000g for 1h of the fraction resulting after precipitation of lysosome and mitochondria. For details see Supplemental Experimental Procedures.

Protein knockdown and mutagenesis

Knock-downs were performed by transduction with lentivirus carrying shRNA against the protein of interest (shRNA sequences are detailed in Supplemental Experimental Procedures). NIH-3T3 fibroblasts knocked down for LAMP-2A were previously described (Massey et al., 2006). The hsc70 and GAPDH mutants were generated using site-directed mutagenesis with the primers detailed under Supplemental Experimental procedures.

Transport assay

Uptake of radiolabeled cytosolic proteins into LE and lysosomes was quantified as described (Kaushik and Cuervo, 2009) upon their incubation with intact isolated organelles as described in Supplemental Experimental procedures.

Proteomic analysis

Cytosol and isolated organelle fractions were separated in a 12% SDS-PAGE, bands were excised, eluted, trypsin digested, and sequenced by microcapillary reverse-phase HPLC nanoelectrospray tandem MS on a Finnigan LCQDECA XP quadruple ion trap mass spectrometer (LCMS/MS). For details see Supplemental Experimental Procedures.

Analysis of hsc70 binding to LE and interaction with lipids

Hsc70 binding to highly purified LE was performed using a fluorescence probe (5-(octadecanoylamino) fluorescein) (MGT Inc.) which is sensitive to the physical and chemical integrity as well as lipid composition of the organelle's limiting membrane (for details see Supplemental Experimental Procedures). The interaction of hsc70 with lipids was analyzed through three different procedures: 1) *Spectrometry:* purified late endosomes labeled with SAF (Stearoyl amino fluoroscein) were incubated with increasing amounts of hsc70 with or without 5mM ATP for 30 minutes at 37°C. Binding of hsc70 was monitored by fluorescence spectroscopy (497nm excitation, 500–550nm emission; 3.3 slit width). 2) *TLC:* Lipid extracts (5μl) were spotted on 0.2mm silica coated plates with fluorescent indicator (polygram sil G/UV 254, from Macherey-Nagel, Duren) and run using a solution of 65:25:1 chloroform: methanol: water as solvent. After the run, the TLC plate was air dried, sprayed with 0.1% Ninhydrin and incubated at 80°C till the purple color developed to identify phosphoserine. 3) *MS/MS:* Lipid extract following immunoprecipitation were analyzed by both MALDI TOF/TOF and LTQ, ESI-TRAP in both MS1 and MS2 modes using a CAD of 35 to identify the head groups and acyl chains (for details see Supplemental Experimental Procedures).

General methods

Immunoblot were developed using standard chemiluminescent procedures after incubation with primary and secondary antibodies as described under Supplemental Experimental

procedures. Transmission electron microscopy analysis were perfomed both in glutharaldehyde/formaldehyde fixed samples and in high pressure frozen cells as described in Supplemental Experimental procedures.

Statistical analysis

All numerical results are reported as mean + s.e.m., and represent data from a minimum of three independent experiments unless otherwise stated. To determine the statistical significance of the difference between experimental groups in instances of multiple means comparisons, we used one-way analysis of variance (ANOVA) followed by the Bonferroni *post-hoc* test. Differences were considered significant for $p<0.05$.

Highlights

- Late endosomes take up cytosolic proteins through membrane invaginations
- Endosomal microautophagy (eMI) requires multivesicular body formation
- Hsc70 mediates selective targeting of cytosolic proteins during eMI
- Hsc70 binds to the endosomal membrane through its polybasic cluster

Supplementary Material

Refer to Web version on PubMed Central for supplementary material.

Acknowledgments

We thank Dr. Erwin Knecht (Instituto the Investigaciones Biomedicas Principe Felipe, Valencia, Spain) for providing the DHFR vector. This work was supported by the National Institute of Health grants AI48833 to LS and AG031782 to AMC and LS and a National Institute on Aging Training Grant (SK).

References

Aniento F, Roche E, Cuervo AM, Knecht E. Uptake and degradation of glyceraldehyde-3- phosphate dehydrogenase by rat liver lysosomes. J Biol Chem. 1993; 268:10463–10470. [PubMed: 8486700]

Arispe N, De Maio A. ATP and ADP modulate a cation channel formed by Hsc70 in acidic phospholipid membranes. J Biol Chem. 2000; 275:30839–30843. [PubMed: 10899168]

Bandyopadhyay U, Kaushik S, Varticovski L, Cuervo AM. The chaperone-mediated autophagy receptor organizes in dynamic protein complexes at the lysosomal membrane. Mol Cell Biol. 2008; 28:5747–5763. [PubMed: 18644871]

Castellino F, Germain RN. Extensive trafficking of MHC class II-invariant chain complexes in the endocytic pathway and appearance of peptide-loaded class II in multiple compartments. Immunity. 1995; 2:73–88. [PubMed: 7600303]

Chiang H, Terlecky S, Plant C, Dice J. A role for a 70 kDa heat shock protein in lysosomal degradation of intracellular protein. Science. 1989; 246:382–385. [PubMed: 2799391]

Cuervo AM. Chaperone-mediated autophagy: selectivity pays off. Trends Endocrinol Metab. 2010; 21:142–150. [PubMed: 19857975]

Cuervo AM, Dice J. A receptor for the selective uptake and degradation of proteins by lysosomes. Science. 1996; 273:501–503. [PubMed: 8662539]

Cuervo AM, Dice J, Knecht E. A lysosomal population responsible for the hsc73-mediated degradation of cytosolic proteins in lysosomes. J Biol Chem. 1997; 272:5606–5615. [PubMed: 9038169]

Dengjel J, Schoor O, Fischer R, Reich M, Kraus M, Muller M, Kreymborg K, Altenberend F, Brandenburg J, Kalbacher H, et al. Autophagy promotes MHC class II presentation of peptides from

intracellular source proteins. Proc Natl Acad Sci U S A. 2005; 102:7922–7927. [PubMed: 15894616]

Dice J. Peptide sequences that target cytosolic proteins for lysosomal proteolysis. Trends Biochem Sci. 1990; 15:305–309. [PubMed: 2204156]

Falguieres T, Luyet PP, Bissig C, Scott CC, Velluz MC, Gruenberg J. In vitro budding of intralumenal vesicles into late endosomes is regulated by Alix and Tsg101. Mol Biol Cell. 2008; 19:4942–4955. [PubMed: 18768755]

Kaushik S, Cuervo AM. Methods to monitor chaperone-mediated autophagy. Methods Enzymol. 2009; 452:297–324. [PubMed: 19200890]

Kunz JB, Schwarz H, Mayer A. Determination of four sequential stages during microautophagy in vitro. J Biol Chem. 2004; 279:9987–9996. [PubMed: 14679207]

Liscum L, Faust JR. The intracellular transport of low density lipoprotein-derived cholesterol is inhibited in Chinese hamster ovary cells cultured with 3-beta-[2-(diethylamino)ethoxy]androst-5-en-17-one. J Biol Chem. 1989; 264:11796–11806. [PubMed: 2745416]

Marzella L, Ahlberg J, Glaumann H. Autophagy, heterophagy, microautophagy and crinophagy as the means for intracellular degradation. Virchows Arch B Cell Pathol Incl Mol Pathol. 1981; 36:219–234. [PubMed: 6116336]

Massey AC, Kaushik S, Sovak G, Kiffin R, Cuervo AM. Consequences of the selective blockage of chaperone-mediated autophagy. Proc Nat Acad Sci USA. 2006; 103:5905–5910. [PubMed: 16585532]

Mizushima N, Levine B, Cuervo AM, Klionsky D. Autophagy fights disease through cellular self-digestion. Nature. 2008; 451:1069–1075. [PubMed: 18305538]

Morshauser RC, Hu W, Wang H, Pang Y, Flynn GC, Zuiderweg ER. High-resolution solution structure of the 18 kDa substrate-binding domain of the mammalian chaperone protein Hsc70. J Mol Biol. 1999; 289:1387–1403. [PubMed: 10373374]

Nimmerjahn F, Milosevic S, Behrends U, Jaffee EM, Pardoll DM, Bornkamm GW, Mautner J. Major histocompatibility complex class II-restricted presentation of a cytosolic antigen by autophagy. Eur J Immunol. 2003; 33:1250–1259. [PubMed: 12731050]

Potolicchio I, Carven GJ, Xu X, Stipp C, Riese RJ, Stern LJ, Santambrogio L. Proteomic analysis of microglia-derived exosomes: metabolic role of the aminopeptidase CD13 in neuropeptide catabolism. J Immunol. 2005; 175:2237–2243. [PubMed: 16081791]

Saksena S, Emr SD. ESCRTs and human disease. Biochem Soc Trans. 2009; 37:167–172. [PubMed: 19143624]

Salvador N, Aguado C, Horst M, Knecht E. Import of a cytosolic protein into lysosomes by chaperone-mediated autophagy depends on its folding state. Journal of Biological Chemistry. 2000; 275:27447–27456. [PubMed: 10862611]

Tanida I, Mizushima N, Kiyooka M, Ohsumi M, Ueno T, Ohsumi Y, Kominami E. Apg7p/Cvt2p: A novel protein-activating enzyme essential for autophagy. Molecular Biology of the Cell. 1999; 10:1367–1379. [PubMed: 10233150]

Wattiaux R, Wattiaux-De Coninck S, Ronveaux-Dupal M, Dubois F. Isolation of rat liver lysosomes by isopycnic centrifugation in a metrizamide gradient. J Cell Biol. 1978; 78:349–368. [PubMed: 211139]

Yeung T, Gilbert GE, Shi J, Silvius J, Kapus A, Grinstein S. Membrane phosphatidylserine regulates surface charge and protein localization. Science. 2008; 319:210–213. [PubMed: 18187657]

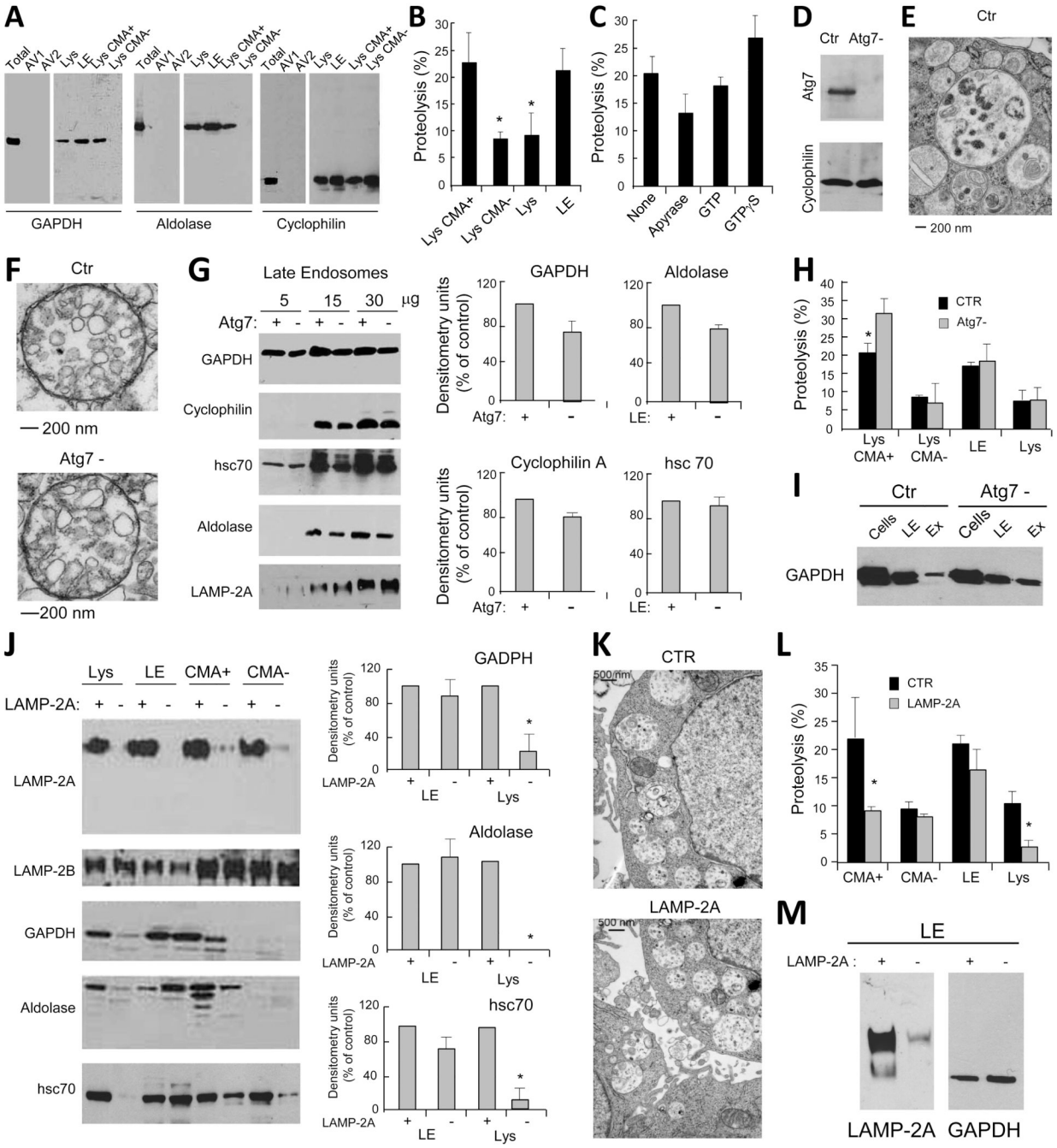

Figure 1. Cytosolic proteins are taken up by late endosomal compartments by mechanisms different from macroautophagy and CMA

(A) Western blot analysis for GAPDH, aldolase and cyclophilin in the indicated purified organelles. **(B)** Degradation (in percentage) of a radiolabeled pool of cytosolic proteins by the indicated intact organelles. Values are mean +S.E. (n = 4). **(C)** Effect of ATP depletion and GTP supplementation on the degradation of a radiolabeled pool of cytosolic proteins by late endosomes. Values were calculated as in B. **(D)** Western blot analysis for Atg7 of control (Ctr) and Atg7 knock down (Atg7-) DC. **(E)** Ultrastructural analysis of autophagosomes in Ctr DC. **(F)** Ultrastructural analysis of purified LE/MVB in Ctr and Atg7- DC. **(G)** Western blot analysis for cytosolic proteins and LAMP-2A of titrated

amounts of purified LE from Ctr and Atg7- DC. *Right:* Densitometric analysis of blots as the one shown here (n= 3). **(H)** Degradation of a radiolabeled pool of cytosolic proteins by the indicated organelles isolated from Ctr and Atg7- DC. Values are mean +S.E. (n = 3). **(I)** Western blot analysis of GAPDH in LE or Exosomes (Ex) isolated from Ctr and Atg7- cells. **(J)** Western blot analysis for LAMP-2 isoforms and cytosolic proteins in fractions from control and LAMP-2A knock down DC. *Right:* Densitometric analysis of blots as the ones shown here (n = 3). **(K)** Ultrastructural analysis of LE/MVB compartments present in Ctr and LAMP-2A(−) cells. **(L)** Degradation of a radiolabeled pool of cytosolic proteins by LE and lysosomes (total, CMA+ and CMA−) from Ctr and LAMP-2A(−) DC. Values are mean +S.E. (n = 3). **(M)** Western blot analysis for the indicated proteins in LE isolated from Ctr (+) and LAMP-2A (−) NIH-3T3 fibroblasts. (*) Significant differences with control values. (See also Fig. S1 and 2).

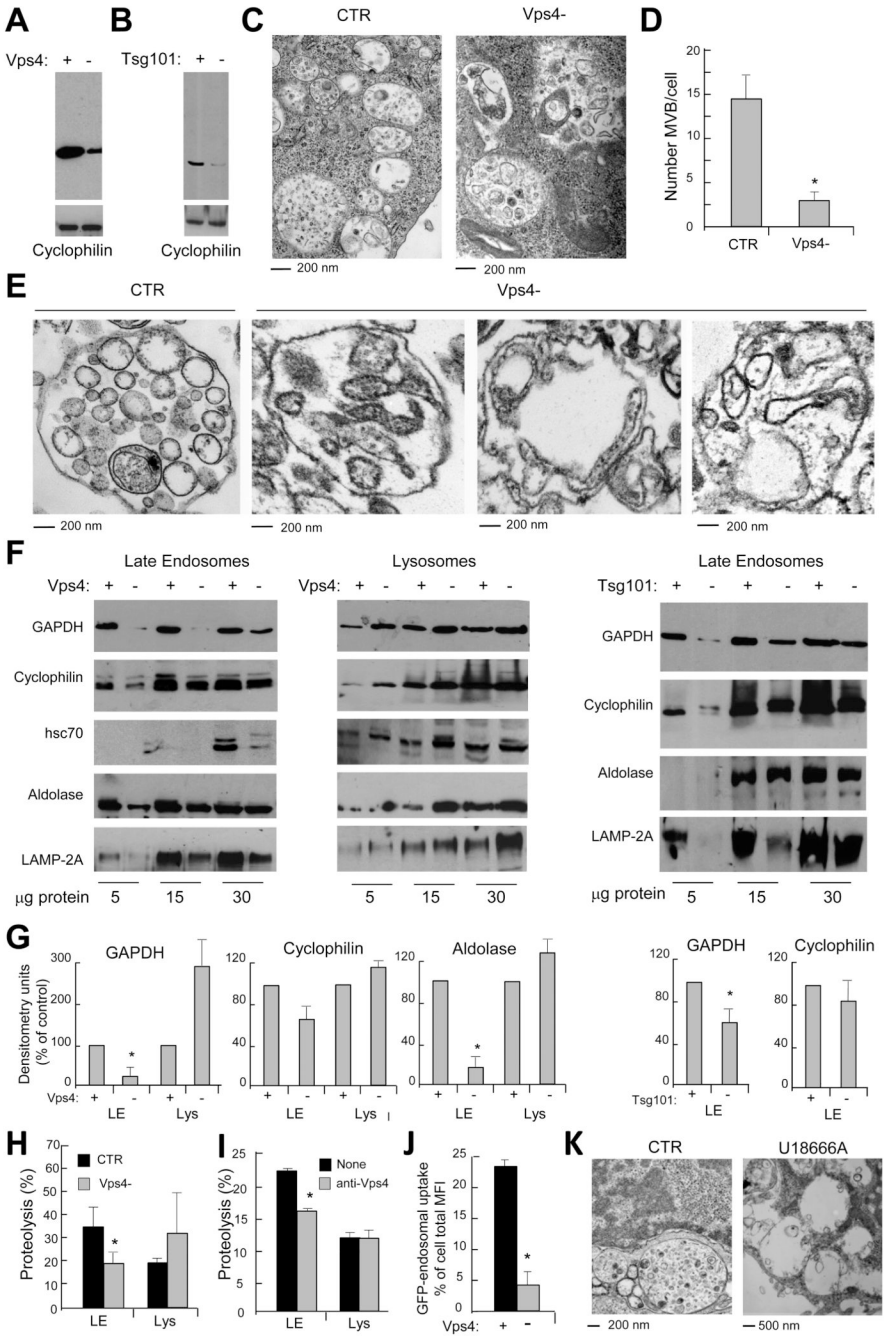

Figure 2. Incorporation of cytosolic proteins into late endosomes requires MVB formation

(A) Western blot analysis for Vps4 of control (+) and Vps4 knock down (−) DC. **(B)** Western blot analysis for Tsg101 of control (+) and Tsg101 knock down (−) DC. **(C)** Ultrastructural analysis of LE/MVB compartments present in Ctr and Vps4- cells. **(D)** Quantification of MVBs in Ctr and Vps4- cells. (*) Significant differences with control/none values. **(E)** Ultrastructural analysis of gradient purified LE/MVB from Ctr and Vps4- DC. **(F)** Western blot analysis for cytosolic proteins and LAMP-2A of titrated amount of gradient purified late endosomes and lysosomes from ctr, Vps4(−) and Tsg101(−)DC. **(G)** Densitometric analysis of western blots as the one show in f. (n = 3) (*) Significant differences with control/none values. **(H)** Degradation (in percentage) of a radiolabeled pool

of cytosolic proteins by late endosomes and lysosomes isolated from Ctr and Vps4- cells. Values are mean +S.E. (n = 3). **(I)** Effect of preincubating endosomes or lysosomes with an antibody against Vps4 in their ability to transport/degrade a pool of radiolabeled cytosolic proteins measure as in h. Values are mean +S.E. (n = 3) (*) Significant differences with control/none values. **(J)** Endosomal uptake of cytosolic GFP. Data are expressed as percentage of endosomal uptake (measured by FACS on purified compartments) calculated over total cellular GFP. (*) Significant differences with control values. **(K)** Ultrastructural analysis of late endosomal multivesicular compartments present in control (CTR) and U18666A treated cells.

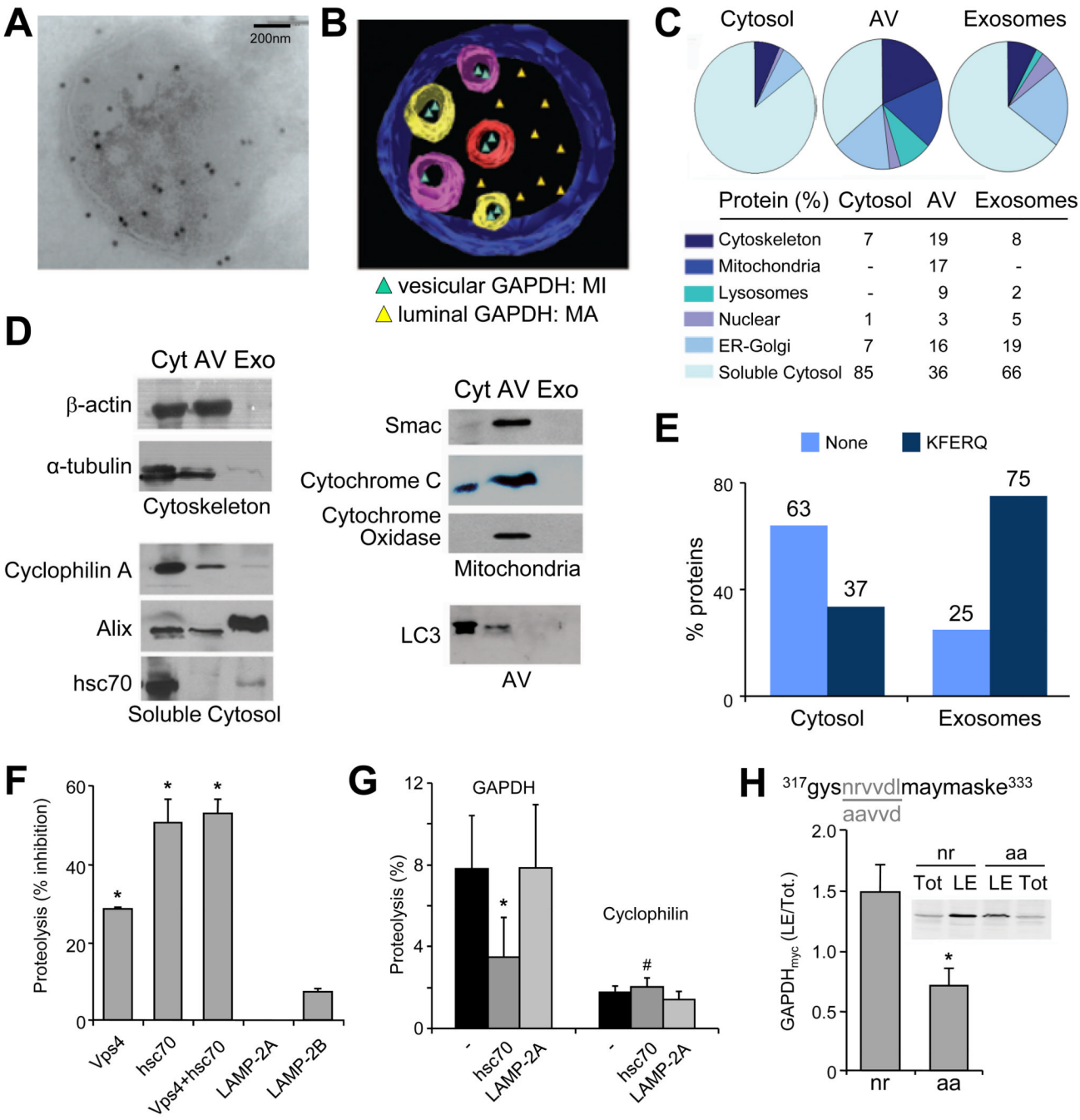

Figure 3. Specific cytosolic proteins are taken up by late endosomes in an hsc70-dependent manner

(A) Immunogold labeling for GAPDH present in a MVB isolated from DC. **(B)** Ultrastructural tomography of a LE/MVB depicting MA-mediated and microautophagy-mediated distribution of cytosolic GAPDH. **(C)** MS/MS analysis and percentage of protein distribution in the soluble cytosol fraction, in purified autophagic vacuoles (AV) and exosomes. **(D)** Western blot analysis of proteins detected in cytosol (Cyt), AV and exosomes (Exo). **(E)** Percentage of proteins containing a KFERQ-like motif distributed among cytosol and exosomes **(F–G)** Effect of preincubating intact LE with the indicated antibodies in their ability to degrade a pool of radiolabeled proteins (**F**) or radiolabeled GAPDH and

cyclophilin (**G**). The inhibitory effect of the different antibodies on proteolysis rates, expressed as %, (**F**) or direct proteolysis values (**G**) are shown. Value are mean +S.E. (n = 3) (*) Significant differences with untreated fractions or control (#) Significant differences with GAPDH. **(H)** Sequences of wild type and amino acid substituted recombinant myc tagged GAPDH (n to a and r to a). Analysis of wild type and mutant $GAPDH_{myc}$ levels in late endosomes. Data are reported as ratio between $GAPDH_{myc}$ (wild type or mutated) in late endosomes (LE) versus total (Tot) in cells. (See also Fig. S3).

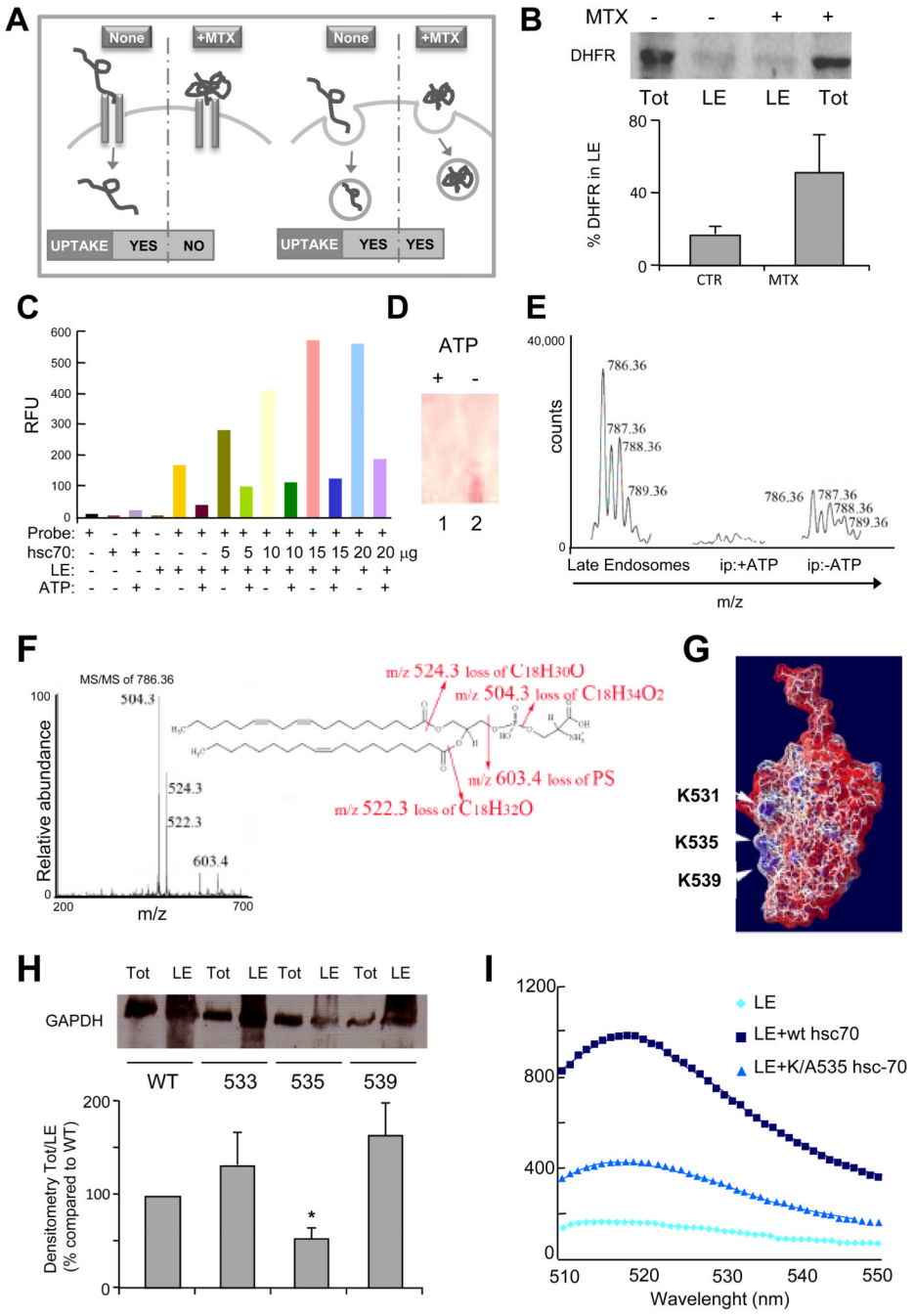

Figure 4. Recruitment of hsc70 to late endosomes is required for endosomal uptake of cytosolic proteins

(A) Western blot analysis of total (Tot) and endosomal (LE) DHFR upon cellular treatment without or with methotrexate (MTX). **(B)** Schematic of hsc70-mediated DHFR translocation in lysosomes (left) and late endosomes (right) in presence and absence of MTX. **(C)** Fluorescence emission scans (excitation wavelength 497 nm, emission scans 510–550 nm) of hsc70 binding to fluorescence labeled LE in presence or absence of ATP. Graphic representation of the fluorescence maximum emission (Λ 520 nm) extrapolated from data reported in Figure S4. Experimental conditions in c and S4 are shown using the same color code. **(D)** Thin layer chromatography (staining with 0.1% ninhydrin) of lipids eluted from

hsc70/LE immunoprecipitation performed in presence or absence of ATP. **(E)** MS analysis of lipids eluted from hsc70/LE immunoprecipitation performed in presence or absence of ATP. **(F)** MS/MS fragmentation of (E) and sequenced phosphatidylserine fragments. A molecular species with an m/z of 786.36 (first peak of the molecular envelope) was detected both in total LE (positive control) and in the hsc70 immunoprecipitate but only in the absence of ATP. **(G)** Electrostatic surface of the C terminal of hsc70 using the color code built in the software Swiss PDB Viewer (red-negative charges (acidic), blue-positive charges (basic) and white-neutral (hydrophobic)). The NMR solved three-dimensional structure of the substrate-binding domain of the mammalian chaperone protein hsc70 was used for all modeling studies (PDB ID: Hsc70)(Morshauser et al., 1999). **(H)** Western blot analysis of hsc70-myc present in late endosomal compartments following transfection of wild type or mutated hsc70. Ratio between total and endosomal hsc70-myc is expressed. **(I)** Fluorescence analysis of wild type and mutant hsc70 binding to LE. (See also Fig. S4).